ARTICLE

Renoprotective effects of tolvaptan in hypertensive heart failure rats depend on renal decongestion

Hiroki Chiba[1] · Yoshihiro Seo[2] · Seika Sai[1] · Mikiko Namekawa[1] · Tomoko Ishizu[2] · Kazutaka Aonuma[2]

Abstract

The vasopressin type 2 receptor antagonist tolvaptan may have renoprotective effects in patients with heart failure (HF). This study aimed to reveal the renoprotective effect of tolvaptan from the viewpoint of hemodynamic combined with catheter and ultrasound examinations in a hypertensive HF model. Dahl salt-sensitive rats ($n = 24$) were fed an 8% high-salt diet after the age of 6 weeks and were treated with tolvaptan ($n = 16$) or vehicle (control group; $n = 8$). The tolvaptan-treated rats were divided into two groups: a low-dose group (0.01% tolvaptan diet; Low-Tol) and a high-dose group (0.05% tolvaptan diet; High-Tol). At 24 weeks, catheterizations to measure central venous pressure (CVP) and renal medullary pressure (RMP) were performed, followed by intrarenal Doppler (IRD) studies and contrast-enhanced ultrasonography (CEUS) to evaluate renal medullary perfusion. The tolvaptan diet reduced CVP (7.7 ± 1.5, 9.0 ± 1.1, and 12.2 ± 0.8 mmHg in the High-Tol, Low-Tol, and control groups, respectively; $p < 0.001$) and RMP (7.7 ± 0.8, 9.4 ± 1.3, and 13.7 ± 1.2 mmHg in the High-Tol, Low-Tol, and control groups, respectively; $p < 0.001$). Tolvaptan also reduced the venous impedance index (VII) in the IRD analysis (0.18 ± 0.03, 0.26 ± 0.04, and 0.40 ± 0.08 in the High-Tol, Low-Tol, and control groups, respectively; $p < 0.001$), and the time to peak intensity in CEUS (6.0 ± 0.5, 7.3 ± 1.3, 9.8 ± 1.8 s in the High-Tol, Low-Tol, and control groups, respectively; $p < 0.001$). Creatinine clearance (Ccr) was preserved in both the High-Tol and Low-Tol groups compared to the control group (4.80 ± 1.9, 4.24 ± 0.8, and 1.35 ± 0.3 mg/min, respectively; $p = 0.001$). Ccr was negatively correlated with RMP ($R = -0.76$, $P < 0.001$), the venous impedance index ($R = -0.70$, $p < 0.001$), time to peak intensity ($R = -0.75$, $P < 0.001$), and renal fibrosis ($R = -0.70$, $p < 0.001$). In contrast, Ccr had modest correlations with systolic blood pressure ($R = -0.50$, $P = 0.02$) and left ventricular ejection fraction ($R = 0.48$, $P = 0.03$). This study revealed that the renoprotective effects of tolvaptan in a hypertensive HF model depended on renal decongestion.

Keywords Tolvaptan · Renal function · Renal congestion · Heart failure

✉ Yoshihiro Seo
  yo-seo@md.tsukuba.ac.jp

[1] Graduate School of Comprehensive Human Sciences, University of Tsukuba, Tsukuba, Japan

[2] Department of Cardiology, Faculty of Medicine, University of Tsukuba, Tsukuba, Japan

Introduction

The vasopressin type 2 receptor antagonist tolvaptan has been used as a diuretic to treat congestive heart failure (HF) in Japan in addition to being approved for use to treat hypovolemic and euvolemic hyponatremia in patients with HF in western countries [1]. Diuretics, including loop and thiazide diuretics, often cause worsening renal function, which is associated with poor outcomes in HF patients [2]. In contrast, tolvaptan may preserve renal function in HF patients. In the Efficacy of Vasopressin Antagonism in Heart Failure Outcome Study With Tolvaptan (EVEREST) trial, tolvaptan did not cause significant changes in renal function compared to the placebo [3], a finding that has been supported in subsequent studies [4–6].

As renal congestion is known as the determinant of WRF in HF patients [7], renal decongestion has been proposed as
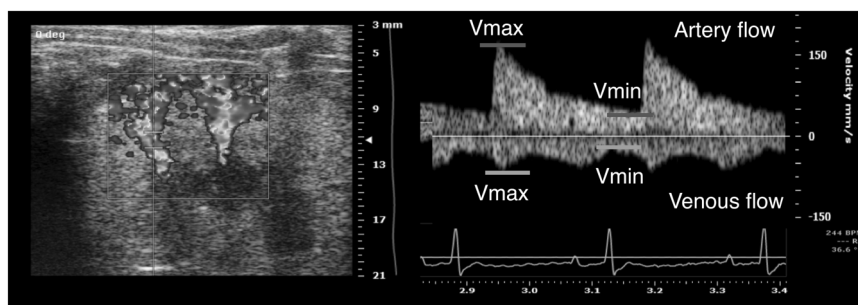
Fig. 1 Doppler flow of renal interlobar vessels The left panel shows a color Doppler image of intrarenal vessels. The sample volume is located on the renal interlobar vessels. The right panel shows the Doppler flow of a renal interlobar artery recorded as a positive signal and that of an interlobar vein recorded as a negative one. Vmax = maximum velocity; Vmin = minimum velocity (color figure online)

one of the mechanisms by which tolvaptan protects renal function [6]. However, the hemodynamic mechanisms of tolvaptan have not been well studied.

We recently demonstrated that real-time contrast-enhanced ultrasonography (CEUS) and pulsed Doppler waveforms of the interlobar arteries and veins, the results of which were validated with catheter hemodynamic evaluation, are useful in assessing renal congestion [8, 9]. This study aimed to reveal the renoprotective effect of tolvaptan through hemodynamic examination combined with catheter and ultrasound studies.

Methods

Experimental animals

In this study, 24 male Dahl salt-sensitive rats, a well-validated model of HF with preserved EF attributable to hypertension (DIS/Eis; Japan SLC, Inc., Shizuoka, Japan), were used. All applicable international, national, and institutional guidelines for the care and use of animals were followed. Animals were treated under an experimental protocol approved by the University of Tsukuba's Institutional Animal Care and Use Committee and in compliance with the Guide for the Care and Use of Laboratory Animals. Dahl salt-sensitive rats ($n = 24$) were fed an 8% NaCl chow diet after the age of 6 weeks and were chronically treated with tolvaptan ($n = 16$) or vehicle (control group: $n = 8$). The tolvaptan-treated rats were divided into two groups, a low-dose group (0.01% tolvaptan diet: Low-Tol) and a high-dose group (0.05% tolvaptan diet; High-Tol), for assessment of the differences in renoprotective effects based on the dose of tolvaptan. Blood pressure measurement by a tail-cuff system (CODA standard system, Hakubatec Lifescience Solutions Co., Ltd., Tokyo, Japan) was performed every 2 weeks from 6 weeks of age.

Echocardiographic studies

Echocardiographic studies were performed every two weeks based on a method described elsewhere [10]. Rats were first anesthetized using isoflurane adjusted to a dose to maintain the heart rate at 300–350 beats per minute. Cardiac image sequences were acquired with a Vevo2100 (VisualSonics Inc., Toronto, Canada) using a 13-24-MHz linear transducer (MS-250). From a parasternal long-axis and a short-axis view, the wall thickness (WT) and left ventricular (LV) diameters were measured, and the LV ejection fraction was estimated by the Teichholz method.

Intrarenal Doppler (IRD) ultrasound

IRD ultrasound studies were performed after the echocardiographic studies. A pulsed sample volume was placed at the renal interlobar vessels under color Doppler flow guidance (Fig. 1) [9]. Pulsed Doppler waveforms of the interlobar arteries and veins were recorded simultaneously. The resistance index (RI) at a lobar artery was calculated as the difference between maximum flow velocity and diastolic flow velocity divided by maximum flow velocity [11]. The venous impedance index (VII) was calculated as the difference between peak maximum flow velocity and maximum flow velocity at nadir divided by peak maximum flow velocity [12].

Hemodynamic studies

When the rats were 24 weeks old, renal medullary pressure (RMP) was measured to assess the increased interstitial pressure caused by medullary edema and increased central venous pressure (CVP) [8]. Rats were anesthetized with isoflurane at a dose adjusted to maintain the heart rate at 300–350 beats per minute. The animals were placed on a heated surgical platform, and the femoral vein was
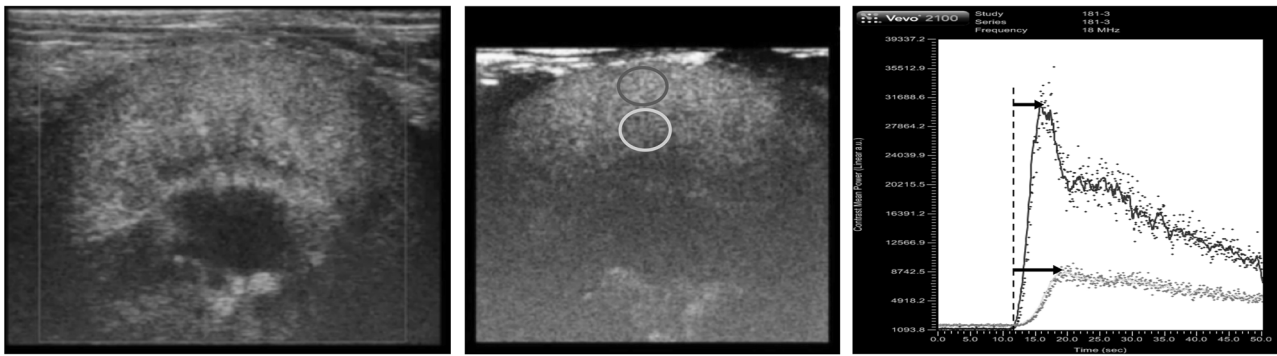
Fig. 2 Contrast-enhanced ultrasonography The center panel shows real-time contrast-enhanced ultrasonographic imaging corresponding to the B-mode imaging in the left panel. In the center panel, the pink circle shows a region of interest in the cortex, and the light blue circle shows a region of interest in the medulla. In the right panel, time-intensity curves are shown. The pink curve is from the cortex region, and the light blue curve is from the medulla. The time from the dashed line located at the starting point of the ascending curve to the peak intensity is measured as the time to peak on each time-intensity curve, as indicated by the arrows (color figure online)

cannulated with a 24-gauge indwelling catheter. A y-connecting catheter was attached to the indwelling catheter for simultaneous direct monitoring of CVP and bolus injection of solutions into the femoral vein. A fiber-optic pressure sensor (FISO-LS-PT9; FISO Technologies, Quebec, Canada) was inserted via the inferior vena cava for continuous monitoring of CVP. The left kidney was exposed, and the other fiber-optic pressure sensor was inserted into the renal medulla to measure RMP. First, a 25-G puncture needle was added to the renal medulla under echo guiding; after removing the stylet, the guide needle was fixed, and a fiber-optic pressure sensor catheter adjusted to zero at atmospheric pressure was inserted.

The tip of the catheter was fixed to the renal medulla with ultrasound image guidance, and both CVP and RMP were continuously monitored by each conditioner module (FISO-LS-10; FISO Technologies). After the catheter was inserted, it was allowed to stand for 5 min, and the values were read when the waveform had stabilized.

Real-time contrast-enhanced ultrasonography (CEUS) studies were performed to visualize and quantify the circulation of peritubular capillaries in the medulla, since we hypothesized that increased medullary pressure due to edema and venous hypertension might cause disturbance of peritubular capillary blood flow [8]. The CEUS studies were also performed with a Vevo2100 system. CEUS was conducted in the kidney that was not catheterized for BMP measurements. An perfluorobutane microbubble ultrasound contrast agent (Daiichi-Sankyo Co. Ltd., Tokyo, Japan) was injected intravenously as a bolus of 0.5 μL into a short extension line followed by flushing 10 mL of saline for 30 s [8, 13] (Supplementary Figure).

The regions of interest (ROIs) were always drawn close to the focal zone, where the enhancement was most homogeneous (Fig. 2). Oval-shaped ROIs were drawn over the mid-superficial outer renal cortex, and the ROIs were placed at a similar depth on the kidney medulla for each subject while avoiding inclusion of the arteries. A time-intensity curve was generated from the average signal intensity in dB obtained within an ROI. On a time-intensity curve, time to peak (TTP, s), which was defined as the time from initial rise to peak, was measured.

Urine and serum measurements

All rats were housed in metabolic cages (CT-10S type II; CLEA Japan, Inc., Tokyo, Japan) to collect urinary samples for 24 h at week 24. The collected urine was used for measurement of urine parameters, including protein, creatinine, sodium, and potassium levels. At week 24, the collected serum from trunk blood was used for analysis of serum parameters including sodium, potassium, urea nitrogen, creatinine, plasma renin activity, angiotensin II, and aldosterone levels.

Renal tissue norepinephrine

Frozen kidneys were homogenized in ice-cold 0.3 N perchloric acid. The homogenate was centrifuged at $18,600 \times g$ for 20 min (Avanti HP-25; Beckman Coulter, Inc., CA, USA); the supernatant was stored at −80 °C until analysis. The renal tissue norepinephrine concentration was determined by high-performance liquid chromatography. The renal tissue norepinephrine concentration (ng/g kidney) was calculated as follows: renal tissue norepinephrine concentration (ng/mL) × homogenate volume (mL)/kidney weight (g) [14].

Histological examination

In addition to body weight, the weights of the excised heart, lung, and kidney were measured for each rat. A kidney that was not catheterized for BMP measurements was fixed with
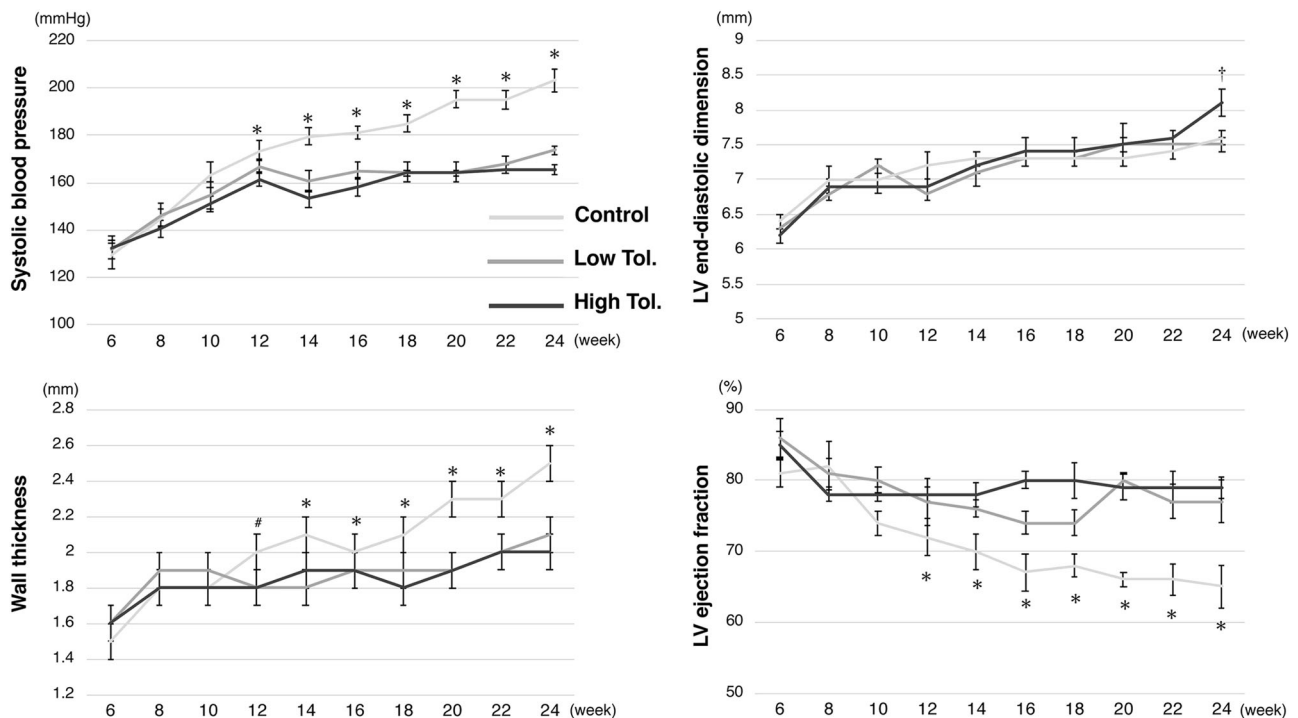
Fig. 3 Changes in systolic blood pressure and left ventricular parameters. The data are shown as the mean ± SEM. LV left ventricular, Tol tolvaptan *$p < 0.05$ vs. data at the same time point in both the Low-Tol and High-Tol groups. #$p < 0.05$ vs. data at the same time point in the High-Tol group. †$p < 0.05$ vs. data at the same time point in the control group

10% formaldehyde. Pathological specimens were stained with Masson's trichrome or hematoxylin-eosin stain for light microscopy (BZ-8100; Keyence, Osaka, Japan). The distribution of the percent area of fibrosis (% area fibrosis) was calculated as the total area of fibrosis (defined as the amount of collagen deposition stained with aniline blue) divided by the entire tissue area.

Statistical analysis

A mean of three measurements was used a surrogate value in each data set. The data are shown as the mean ± standard error or as the mean ± standard deviation. One-way analysis of variance (ANOVA) with a post hoc Tukey–Kramer test was used to compare continuous variables among three groups. Changes among repeated measurements were evaluated using a linear mixed model analysis with a post hoc Bonferroni test. Correlations between parameters were evaluated by Pearson's correlation coefficient. A value of $p < 0.05$ was considered statistically significant. All statistical analyses were performed using SPSS software (version 25.0, SPSS Inc., Chicago, IL).

Results

Initial measurements were obtained from all 24 rats. One rat in the Low-Tol group died spontaneously at 18 weeks and

thus did not complete the experimental protocol. The cause of death was not investigated.

The high-salt diet induced significant and sustained elevations in systolic blood pressure (SBP) after week 12 (Fig. 3). SBP was significantly higher in the control group than in both the Low-Tol and High-Tol groups at each time point.

WT in the control group showed a significant and sustained increase starting at week 12 compared to week 6 ($p < 0.05$). In contrast, WT in the Low-Tol group did not change after week 10, and that in the High-Tol group did not change after week 12. As a result, WT in the control group was significantly higher than that in both the Low-Tol and High-Tol groups from week 14 onward. LV end-diastolic dimensions did not differ between the tolvaptan groups and the control group at any week except in the High-Tol group at week 24.

LV ejection fraction in the control group was reduced at week 16 compared to week 6 ($p < 0.01$). Since LV ejection fraction did not change significantly throughout the experimental period in either the Low-Tol and High-Tol groups, LV ejection fraction in the control group was significantly lower than that at each time point in both the Low-Tol and High-Tol groups.

IRD flow

Representative cases from the control and High-Tol groups are shown in Fig. 4.
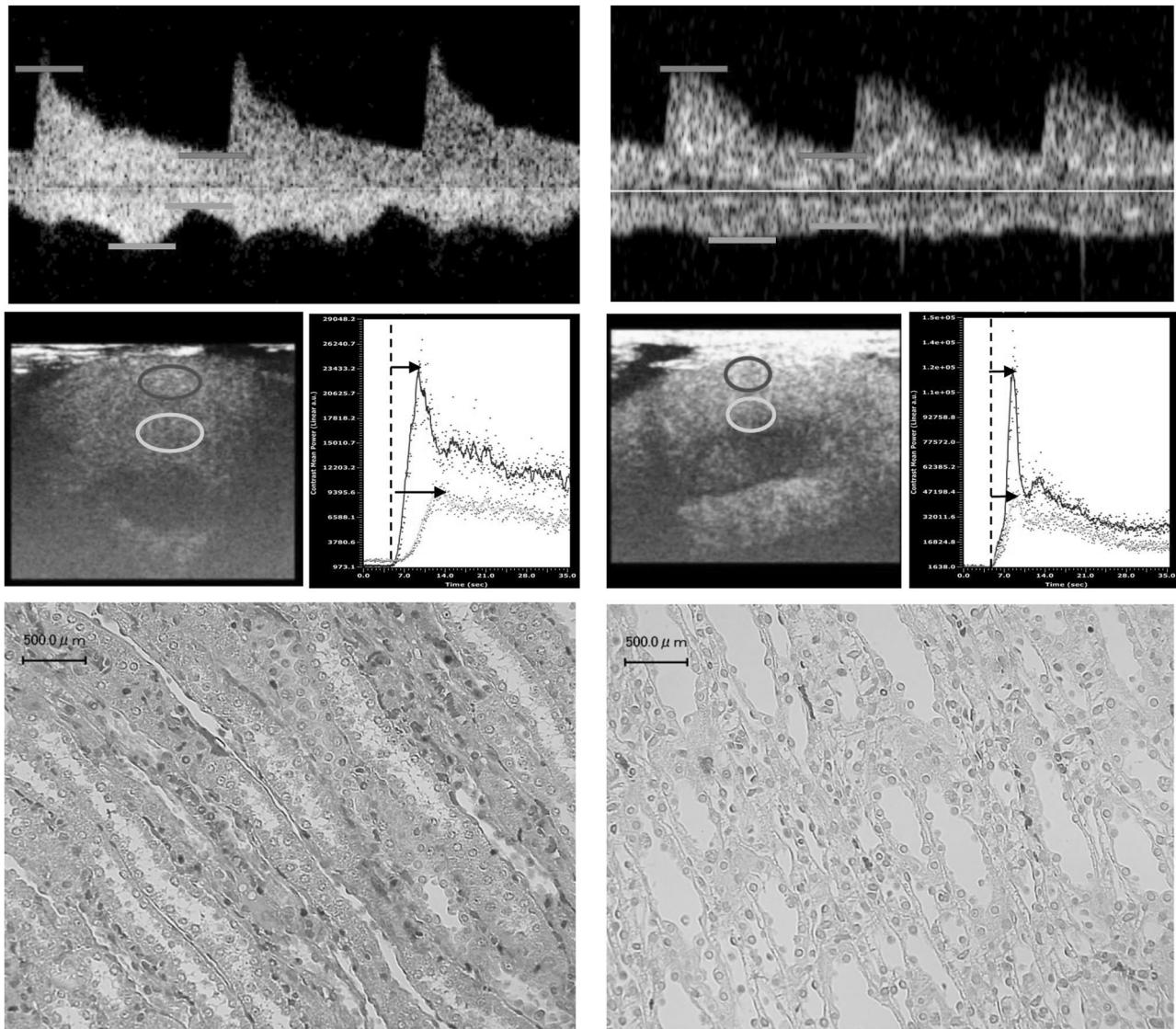
Fig. 4 Comparisons between the control and high-dose tolvaptan groups. Representative datasets of the control and high-dose tolvaptan (High-Tol) groups are shown. The left panels are derived from a control rat, and the right panels are derived from a rat in the High-Tol group. Each upper panel shows the Doppler flow of renal interlobar vessels at week 24. Unlike the Doppler flow of the interlobar vein from the control rat, the flow of that from the rat in the High-Tol group was almost steady (control VII = 0.7; High-Tol VII = 0.2). In each middle panel, time-intensity curves are shown. Time to peak (TTP) on the time-intensity curve for the medulla of the control rat (left panel, light blue curve) is markedly longer than TTP of the rat in the High-Tol group (right panel, light blue curve) (control medulla TTP = 9.7 s; High-Tol medulla TTP = 5.6 s). Each lower panel shows an image of tubulointerstitial sections in the medulla with Masson's trichrome staining. The fibrotic area of the control rat is more marked than that of the rat in the High-Tol group (control percent area of fibrosis = 25%; High-Tol percent area of fibrosis = 5%) (color figure online)

Fig. 5 Changes in interlobar Doppler flow parameters. The data are shown as the mean ± SEM. *$p < 0.05$ vs. data at the same time point in both the Low-Tol and High-Tol groups. #$p < 0.05$ vs. data at the same time point in the High-Tol group. †$p < 0.05$ vs. data at the same time point in the control group
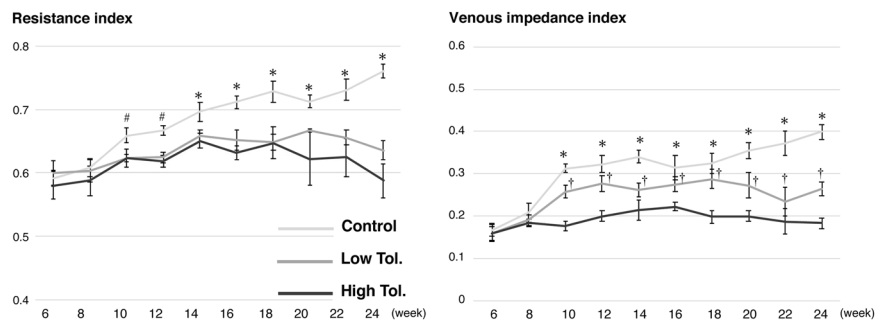
Table 1 Characteristics in examinations at week 24

	Control	Low-Tol	High-Tol	P value
Hemodynamics				
SBP, mmHg	206 ± 8.3*	191 ± 15	191 ± 7.9	0.02
Heart rate, bpm	402 ± 25	380 ± 25	404 ± 30	0.20
CVP, mmHg	12.2 ± 0.8#	9.0 ± 1.1	7.7 ± 1.5	<0.001
RMP, mmHg	13.7 ± 1.2#	9.4 ± 1.3†	7.7 ± 0.8	<0.001
Intra-renal echo				
RI	0.76 ± 0.07#	0.64 ± 0.04	0.58 ± 0.05	<0.001
VII	0.40 ± 0.08#	0.26 ± 0.04†	0.18 ± 0.03	<0.001
TTP in cortex, s	4.3 ± 0.8	5.0 ± 1.2	4.2 ± 1.0	0.07
TTP in medulla, s	9.8 ± 1.8#	7.3 ± 1.3†	6.0 ± 0.5	<0.001
Histopathology				
Body weight, g	423 ± 5.6	422 ± 6.7	414 ± 10.4	0.10
Heart, g	1.55 ± 0.13*	1.34 ± 0.08	1.33 ± 0.14	0.03
Lung, g	2.04 ± 0.21*	1.69 ± 0.28	1.64 ± 0.22	0.01
Kidney, g	1.82 ± 0.16*	1.69 ± 0.11	1.53 ± 0.16	0.009
Percent area of fibrosis, %	20.6 ± 3.5#	11.3 ± 1.0	8.0 ± 2.6	<0.001
Serum parameters				
Sodium, mEq/L	147 ± 1.9	147 ± 1.7	146 ± 2.3	0.87
Potassium, mEq/L	4.1 ± 0.5	3.8 ± 0.3	4.0 ± 1.1	0.61
BUN, mg/dL	48 ± 3.9*	40 ± 2.8	38 ± 3.3	0.007
Creatinine, mg/dL	0.96 ± 0.04#	0.55 ± 0.02†	0.48 ± 0.05	<0.001
PRA, pg/mL/h	0.48 ± 0.15#	2.36 ± 0.76	2.44 ± 0.91	<0.001
Aldosterone, pg/mL	216 ± 57	220 ± 37	193 ± 49	0.56
Urine parameters				
UV, mL/day	37 ± 11	36 ± 14	43 ± 24	0.72
Sodium, mEq/L	394 ± 40#	72 ± 20	96 ± 24	<0.001
Creatinine, mg/dL	30.0 ± 5.0#	95.5 ± 30.2	86.8 ± 34.6	0.001
Protein, mg/dL	166 ± 17.2	173 ± 41	121 ± 44	0.08
Ccr, mg/min	1.35 ± 0.3#	4.24 ± 0.8	4.80 ± 1.9	0.001
Tissue parameters				
Renal norepinephrine, ng/g kidney	33.2 ± 24.7	34.3 ± 7.3	32.9 ± 4.4	0.26

Data is shown as mean ± SD

BUN blood urea nitrogen, *Ccr* creatinine clearance, *CVP* central venous pressure, *PRA* plasma renin activity, *RI* resistance index, *RMP* renal medullary pressure, *SBP* systolic blood pressure, *Tol* tolvaptan, *TTP* time to peak on a time-intensity curve, *UV* urine volume, *VII* venous impedance index

*$p < 0.05$ vs. others, #$p < 0.01$ vs. others, †$p < 0.05$ vs. High-Tol

The RI in the control group was significantly increased from week 10 onward compared to week 6 and showed sustained elevation throughout the observation period (Fig. 5). The RI at week 24 was significantly higher than that from weeks 6 to 18 ($P < 0.001$). The RI in both the Low-Tol and High-Tol groups was increased at week 14 compared to week 6 ($P < 0.05$). The RI in the Low-Tol group did not significantly change from week 14 to 24. In contrast, the RI in the High-Tol group decreased from week 20 to 24, at which point it did not differ from that at week 6. The control group had a higher RI than the Low-Tol group at each point after week 10 and a higher RI than the High-Tol group at each point after week 14.

The VII in the control group was significantly increased from week 8 onward compared to week 6 ($P < 0.01$), increasing gradually until week 22. The VII at week 24 was significantly higher than that between week 6 and week 22 ($p < 0.01$). In the Low-Tol group, compared to week 6, a significant difference in VII was observed starting at week 10 and continuing until week 24 ($p < 0.001$). In contrast, there were no significant alterations in the High-Tol group, as shown by the representative case in Fig. 4. At each point,
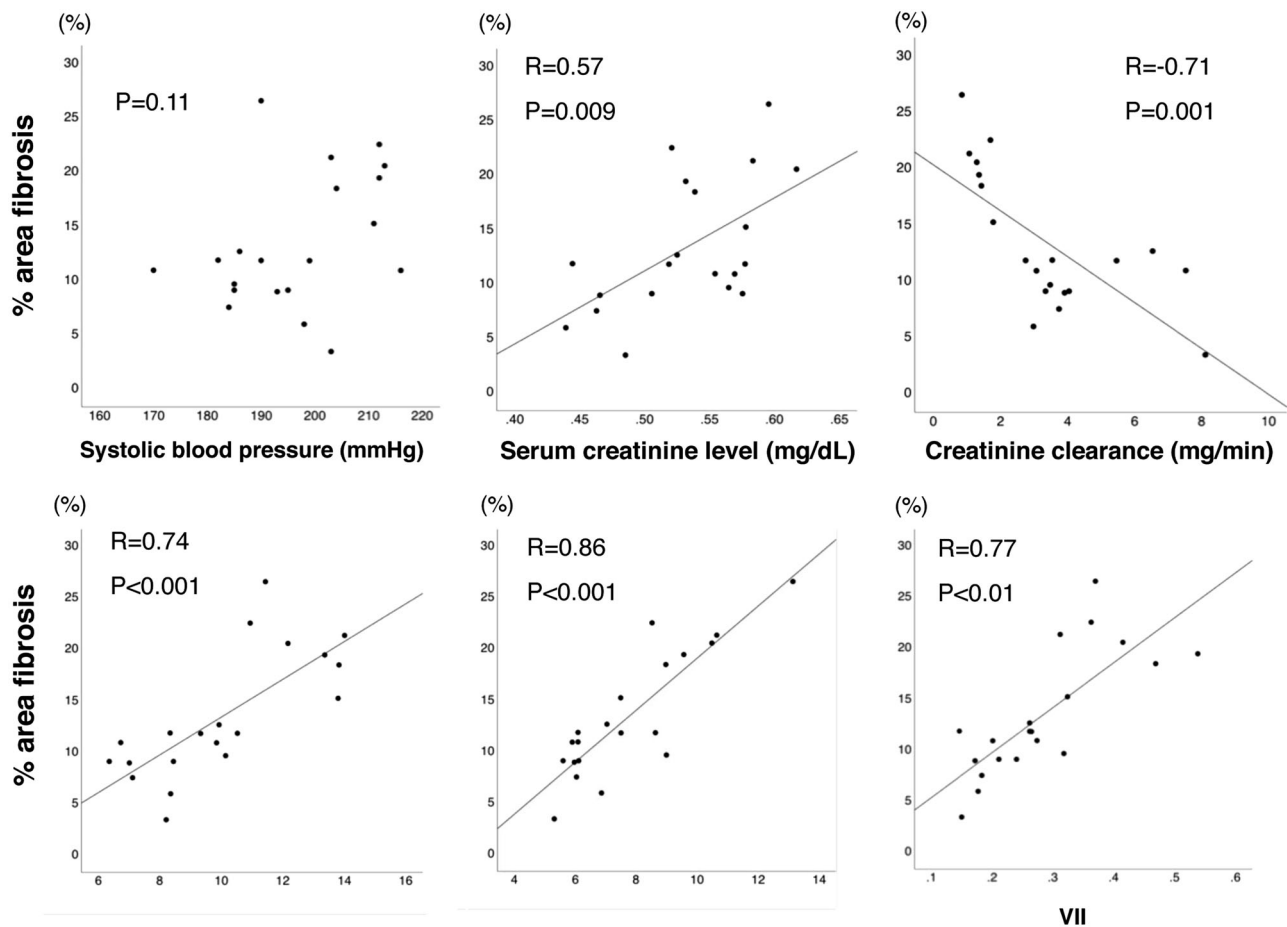
Fig. 6 Correlations between percent area of fibrosis in a tubulointerstitial section and hemodynamic, ultrasound, and laboratory parameters % area fibrosis = percent area of fibrosis, RMP renal medullary pressure, TTP time to peak on a time-intensity curve, VII venous impedance index

the VII in the control group was significantly higher than that in both the Low-Tol and High-Tol groups from week 10 onward. In addition, there were significant differences between the Low-Tol and the High-Tol groups from week 10 onward.

Examinations at week 24

All data from examinations at week 24 are summarized in the Table 1. In all rats, RMP was closely correlated with CVP ($R = 0.82$, $Y = 0.9 \times + 1.2$, $p < 0.001$). Both CVP and RMP in the control group were significantly higher than those in the Low-Tol and High-Tol groups. Despite the lack of a significant difference in CVP between the Low-Tol and the High-Tol groups, RMP in the High-Tol group was significantly lower than that in the Low-Tol group.

In the CEUS examinations, TTP in the medulla differed among groups, but not that in the cortex. In addition, TTP in the High-Tol group was significantly shorter than that in the Low-Tol group.

Regarding the serum parameters, BUN and creatinine levels in the control group were higher than those in the High-Tol group. In addition, creatinine levels in the Low-Tol group were significantly higher than those in the High-Tol group.

Plasma renin activity (PRA) in the control group was significantly lower than that in the Low-Tol and High-Tol groups. However, aldosterone levels did not differ among the groups, nor did renal tissue norepinephrine levels.

In the control group, urinary sodium excretion was markedly increased compared to that in the Low-Tol and the High-Tol groups. Creatinine clearance (Ccr) in the control group was significantly lower than that in the Low-Tol and the High-Tol groups. Ccr was significantly and negatively correlated with CVP ($R = -0.78$, $P < 0.001$), RMP ($R = -0.76$, $P < 0.001$), the RI ($R = -0.65$, $P <$

0.001), the VII ($R = -0.70$, $p < 0.001$), TTP in the medulla ($R = -0.75$, $P < 0.001$), and renal fibrosis ($R = -0.70$, $p < 0.001$). In contrast, SBP had a significant but modest correlation with Ccr ($R = -0.50$, $P = 0.02$), and LVEF modestly correlated with Ccr ($R = 0.48$, $P = 0.03$).

In histopathological studies, the weights of the heart, lung, and kidney in the control group were significantly higher than those in the Low-Tol and the High-Tol groups, although body weight did not differ among the groups. The % area fibrosis was also significantly increased in the control group compared to the Low-Tol and the High-Tol groups, as shown in Fig. 4.

The % area fibrosis significantly correlated with RMP, TTP in the medulla, and the VII despite no significant correlation with SBP (Fig. 6). Regarding renal function, creatinine levels had a positive correlation and Ccr had a negative correlation with the % area fibrosis. Renal tissue norepinephrine levels and plasma aldosterone levels showed no significant correlation with the % area fibrosis. In contrast, PRA negatively correlated with % area fibrosis.

Discussion

This study showed that renal hemodynamic changes occurred due to tolvaptan administration. In addition, inhibition of renal congestion by tolvaptan was associated with the renoprotective effect. To the best of our knowledge, the present study is the first to demonstrate the relationship between the renoprotective impact of tolvaptan and intrarenal hemodynamic changes using a HF rat model.

Imaging for renal congestion

This study revealed differences in intrarenal hemodynamics between chronic HF models with and without tolvaptan administration. Renal congestion has been an issue of focus for cardiorenal syndrome in HF patients, and imaging studies have not been sufficiently performed. Previous studies have shown and this study also confirmed increases in intrarenal pressure accompanied by CVP increases, which suggests that edema from renal congestion causes intrarenal pressure to increase because the kidneys are encapsulated organs [15]. The increased interstitial pressure may directly compress vessels in the renal medullary regions and reduce vessel capacitance or compliance; we previously reported the usefulness of CEUS for assessments of medullary circulation and Doppler examinations of intrarenal lobar vessels [8, 9].

Renoprotective effects of tolvaptan

Our series showed significantly lower SBP in the tolvaptan groups than in the HF model group without tolvaptan. This

observation disagrees with a previous report [16]. However, the present study started tolvaptan administration after week six, before the LV hypertrophy stage. In addition, although serum sodium levels did not differ among the groups, the markedly increased urinary sodium excretion in the control group may be associated with increased RMP. The findings are supported by the fact that renal interstitial hydrostatic pressure is a determinant of urinary sodium excretion [17]. Therefore, an aggressively decreased preload independent of natriuresis may be associated with lower BP in the tolvaptan groups, which might also be supported by the observed increases in PRA. Additionally, LV hypertrophy was inhibited and LVEF was preserved in the tolvaptan groups, an effect also related to the beneficial hemodynamic effects of tolvaptan. However, these effects did not have the strongest impact in the protection of renal function. Instead, renal parameters associated with renal congestion had closer relationships with Ccr.

In addition, renal fibrosis was significantly inhibited in the tolvaptan-treated groups compared to the control group. The % area fibrosis was significantly correlated with renal function and hemodynamic and ultrasound parameters of the medulla. These findings suggest a close relationship between renal fibrosis and renal congestion in addition to the close relationship between renal fibrosis and renal function. In contrast, the % area fibrosis was not correlated with SBP, renal tissue norepinephrine levels, or plasma aldosterone levels. Furthermore, PRA was rather negatively correlated with fibrosis rate, supporting the idea that increased PRA is associated with hemodynamic changes due to decongestion. There has been growing interest in inflammatory and endothelial cell activation by venous congestion [18, 19]. In the future, we will study the relationship between renal congestion and renal fibrosis through fundamental research.

Renal venous congestion influences the sympathetic nervous system (SNS) and the renin-angiotensin-aldosterone system (RAAS) in acute hemodynamic change models with venous hypertension to 30 mmHg [20, 21]. However, evidence with chronic HF models is unclear. Our data from the chronic HF model suggest that the contributions of the SNS and RAAS are so complex and it is difficult to eliminate the effect of systemic hemodynamic changes, as PRA increased in the tolvaptan-treated groups. In this study, we could not assess HF biomarkers. Recently, Imazu et al. [22] reported that fibroblast growth factor 23 (FGF23) provides beneficial information in patients with right-sided HF and may provide different clinical information than that provided only by plasma B-type natriuretic peptide levels. Since FGF23 is also associated with chronic kidney disease [23], basic studies on this novel biomarker using our renal pathophysiological methods may provide additional information about renal congestion in HF.

In summary, renal decongestion, rather than blood pressure effects, may be the primary effect of tolvaptan in protecting renal function.

Dose-dependent effects of tolvaptan

RMP, TTP in the medulla, and creatinine levels were significantly lower in the High-Tol group than in the Low-Tol group. We tried to show differences in renoprotective effects based on the dose of tolvaptan, and these results might indicate a dose-dependent renoprotective effect. However, more precise information and analysis are needed to conclude the existence of a dose-dependent effect. Precise measurement of daily food intake should have been performed to estimate the daily intake of tolvaptan. However, we did not measure daily food intake and did not assess the serum concentrations of tolvaptan. Therefore, we cannot conclude that tolvaptan had a dose-dependent renoprotective effect in this study.

Limitations

Tolvaptan administration was started before the LV hypertrophic stage. Therefore, the effects of later administration during the LV hypertrophic or HF stages should be investigated in future studies. Molecular biological analyses were not performed. Thus, further studies are needed to identify the mechanism of the renoprotective effects of tolvaptan mediated by renal decongestion.

In addition, comparisons with loop diuretics were not performed. Tolvaptan may have a stronger effect on interstitial decongestion than loop diuretics. In the future, comparisons are needed to clarify the specific renoprotective effects of tolvaptan mediated by renal decongestion.

Conclusions

The renoprotective effects of tolvaptan in a Dahl hypertensive HF model depended on renal decongestion. Further studies are needed to reveal the pathophysiological mechanisms.

Compliance with ethical standards

References

1. Fukunami M, Matsuzaki M, Hori M, Izumi T. Tolvaptan Investigators. Efficacy and safety of tolvaptan in heart failure patients with sustained volume overload despite the use of conventional diuretics: a phase III open-label study. Cardiovasc Drugs Ther. 2011;25(Suppl 1):S47–56.

2. Damman K, Valente MA, Voors AA, O'Connor CM, van Veldhuisen DJ, Hillege HL. Renal impairment, worsening renal function, and outcome in patients with heart failure: an updated meta-analysis. Eur Heart J. 2014;35:455–69.

3. Gheorghiade M, Konstam MA, Burnett JC Jr, Grinfeld L, Maggioni AP, Swedberg K, et al. Efficacy of Vasopressin Antagonism in Heart Failure Outcome Study With Tolvaptan (EVEREST) Investigators. Short-term clinical effects of tolvaptan, an oral vasopressin antagonist, in patients hospitalized for heart failure: the EVEREST Clinical Status Trials. JAMA. 2007;297:1332–43.

4. Matsue Y, Suzuki M, Seya M, Iwatsuka R, Mizukami A, Nagahori W, et al. Tolvaptan reduces the risk of worsening renal function in patients with acute decompensated heart failure in high-risk population. J Cardiol. 2013;61:169–74.

5. Kimura K, Momose T, Hasegawa T, Morita T, Misawa T, Motoki H, et al. Early administration of tolvaptan preserves renal function in elderly patients with acute decompensated heart failure. J Cardiol. 2016;67:399–405.

6. Sen J, Chun E, McGill D. Tolvaptan for heart failure in chronic kidney disease patients: a systematic review and meta-analysis. Heart Lung Circ. (epub ahead of print 13 2018; https://doi.org/10.1016/j.hlc.2017.12.013).

7. Damman K, van Deursen VM, Navis G, Voors AA, van Veldhuisen DJ, Hillege HL. Increased central venous pressure is associated with impaired renal function and mortality in a broad spectrum of patients with cardiovascular disease. J Am Coll Cardiol. 2009;53:582–8.

8. Komuro K, Seo Y, Yamamoto M, Sai S, Ishizu T, Shimazu K, et al. Assessment of renal perfusion impairment in a rat model of acute renal congestion using contrast-enhanced ultrasonography. Heart Vessels. 2018;33:434–40.

9. Seo Y, Nakatsukasa T, Sai S, Ishizu T, Iida N, Yamamoto M, et al. Clinical implications of organ congestion in heart failure patients as assessed by ultrasonography. Cardiovasc Diagn Ther. 2018;8:57–69.

10. Koshizuka R, Ishizu T, Kameda Y, Kawamura R, Seo Y, Aonuma K. Longitudinal strain impairment as a marker of the progression of heart failure with preserved ejection fraction in a rat model. J Am Soc Echocardiogr. 2013;26:316–23.

11. Platt JF, Ellis JH, Rubin JM, DiPietro MA, Sedman AB. Intrarenal arterial Doppler sonogra- phy in patients with nonobstructive renal disease: correlation of resistive index with biopsy findings. Am J Roentgenol. 1990;154:1223–7.

12. Ishimura E, Nishizawa Y, Kawagishi T, Okuno Y, Kogawa K, Fukumoto S, et al. Intrarenal hemodynamic abnormalities in diabetic nephropathy measured by duplex Doppler sonography. Kidney Int. 1997;51:1920–7.

13. Watanabe R, Matsumura M, Chen CJ, Kaneda Y, Ishihara M, Fujimaki M. Gray-scale liver enhancement with Sonazoid (NC100100), a novel ultrasound contrast agent; detection of hepatic tumors in a rabbit model. Biol Pharm Bull. 2003;26:1272–7.

14. Machino T, Murakoshi N, Sato A, Xu D, Hoshi T, Kimura T, et al. Anti-hypertensive effect of radiofrequency renal denervation in spontaneously hypertensive rats. Life Sci. 2014;110:86–92.

15. Burnett JC Jr, Knox FG. Renal interstitial pressure and sodium excretion during renal vein constriction. Am J Physiol. 1980;238:279–82.

16. Morooka H, Iwanaga Y, Tamaki Y, Takase T, Akahoshi Y, Nakano Y, et al. Chronic administration of oral vasopressin type 2 receptor antagonist tolvaptan exerts both myocardial and renal protective effects in rats with hypertensive heart failure. Circ Heart Fail. 2012;5:484–92.

17. Farrugia E, Lockhart JC, Larson TS. Relation between vasa recta blood flow and renal interstitial hydrostatic pressure during pressure natriuresis. Circ Res. 1992;71:1153–8.

18. Ganda A, Onat D, Demmer RT, Wan E, Vittorio TJ, Sabbah HN, et al. Venous congestion and endothelial cell activation in acute decompensated heart failure. Curr Heart Fail Rep. 2010;7:66–74.

19. Colombo PC, Onat D, Harxhi A, Demmer RT, Hayashi Y, Jelic S, et al. Peripheral venous congestion causes inflammation, neurohormonal, and endothelial cell activation. Eur Heart J. 2014;35:448–54.

20. Kishimoto T, Maekawa M, Abe Y, Yamamoto K. Intrarenal distribution of blood flow and renin release during renal venous pressure elevation. Kidney Int. 1973;4:259–66.

21. Doty JM, Saggi BH, Sugerman HJ, Blocher CR, Pin R, Fakhry I, et al. Effect of increased renal venous pressure on renal function. J Trauma. 1999;47:1000–3.

22. Imazu M, Takahama H, Amaki M, Sugano Y, Ohara T, Hasegawa T, et al. Use of serum fibroblast growth factor 23 vs. plasma B-type natriuretic peptide levels in assessing the pathophysiology of patients with heart failure. Hypertens Res. 2017;40:181–8.

23. Hu MC, Shiizaki K, Kuro-o M, Moe OW. Fibroblast growth factor 23 and Klotho: physiology and pathophysiology of an endocrine network of mineral metabolism. Annu Rev Physiol. 2013;75:503–33.